Food Biophysics
https://doi.org/10.1007/s11483-024-09877-z

RESEARCH

Investigating the Efficacy of Chitosan-Enriched *Cuminum cyminum* Essential Oil Against Food-Borne Molds, Aflatoxin B_1, and Post-Harvest Quality of *Arachis hypogaea* L.

Akshay Kumar[1,2] · Tanya Singh Raghuvanshi[1] · Vishal Gupta[1] · Vivekanand[1] · Niraj Kohar[1] · Bhanu Prakash[1]

Received: 13 June 2024 / Accepted: 7 August 2024

Abstract
Nanoencapsulation of essential oils exhibited promising applications in food industries, especially in controlling spoilage due to food-borne microbes. In this study, the enhanced antimicrobial efficacy of nanoencapsulated *Cuminum cyminum* essential oil (Ne-CEO) against food-borne molds, and aflatoxin B_1 contamination was observed in a dose-dependent manner. The GC-MS results represent 14 different volatile organic compounds of (CEO) (94.49%), where cuminaldehyde was found to be the major one. The interaction of the *Cuminum cyminum* essential oil (CEO) and chitosan nanoparticles (CSNPs) was confirmed with the Scanning Electron Microscopy (SEM) and Fourier Transform Infrared Spectroscopy (FTIR) analysis. The Ne-CEO exhibited superior antimicrobial effects compared to non-encapsulated CEO and inhibited the growth of selected mold species (0.3–0.5 µL/mL) and aflatoxin B_1 (AFB_1) secretion at 0.4 µL/mL. The probable toxicity mechanism results show membrane impairment and cellular homeostasis linked with decreased ergosterol content, increased cation leakage, impairment in antioxidant defenses, carbon metabolism, and transcriptional genes (Ver-1 and Nor-1) functioning of AFB_1 biosynthesis. Furthermore, during the six months in-situ trial, Ne-CEO (0.4 µL/mL) remarkably protected the biodeterioration of *A. hypogaea* seed samples against *A. flavus* growth and AFB_1 contamination, thus enhancing its practical application as a plant-based food preservative to enhance the shelf-life of food commodities.

Keywords Aflatoxin B_1 · *Aspergillus flavus* · Chitosan · *Cuminum cyminum* · Nanoencapsulation

Introduction

Aflatoxin B_1 (AFB_1), a potent carcinogenic metabolite produced by *Aspergillus flavus*, and *A. parasiticus* is often reported as one of the common causes of fungal toxicity in tropical and sub-tropical countries. It is also responsible for hepatocellular carcinoma and has teratogenic, immunosuppressive, and mutagenic effects [1, 2]. Among the four most common types of aflatoxins (AFB_1, AFB_2, AFG_1, and AFG_2), AFB_1 is highly thermostable and considered one of the most common cause of hepatocellular carcinogen (Class 1 category) [3]. Further, fungi may easily infest agri-food products during harvesting, storage, and transportation, and according to the Food and Agriculture Organisation (FAO) reports around 25% of the world's crops are infested with molds and associated mycotoxin contamination causing severe losses up to $1 billion [4].

Arachis hypogaea L. (Peanut) seed samples are rich source of fat, protein, vitamins, and minerals, often prone to *A. flavus* contamination which reduces its nutritional quality and makes it unsafe for consumption either as raw material or in processed form [5]. In general, to prevent mold deterioration synthetic preservatives such as propionic acid, benzoic acid, sorbic acid, nitrate, and their salts were used in the food products by the industries [6, 7]. Recent reports suggested that the prolonged use of these synthetic preservatives could have serious concerns for health (residual toxicity) and the environment (resistance development) [8]. These negative concerns foster the demand for a natural alternative to control molds and AFB_1 in food products,

✉ Bhanu Prakash
bprakash@bhu.ac.in; bhanubhu08@gmail.com

[1] Department of Botany, Institute of Science, Banaras Hindu University, Varanasi 221005, India

[2] Department of Botany, Shri-Ganesh Rai P. G. College, Dobhi-Jaunpur, Uttar Pradesh, India

Published online: 13 August 2024

thus. in the past few years, significant research progress has been made to investigate the potential of traditionally used essential oils as a green chemical agent [9, 10]. Many benefits are often associated with traditionally used plant essential oils such as their eco-friendly nature, relative health benefits, often non-toxic, and proven antimicrobial activity. As a result, the United States Food and Drug Administration (US-FDA) has kept many of them in generally recognised as safe category (GRAS) [11].

In general, essential oils (EOs) harbor antimicrobial, antioxidant, anti-inflammatory, insect-killing, and antiviral properties, hence, could be used as novel sources of green chemical agents with diverse antimicrobial mechanisms. However, the applications of EOs have not yet been widely explored due to certain hurdles related to low water solubility, intense volatility, negative effects on sensory attributes, and instability in the food matrix [12, 13]. However, the recent green nanotechnology approach, which integrates nanotechnology with sustainable chemistry ideas and techniques, could be used to address the limitations above of EOs. Literature survey revealed that nanoencapsulated essential oils often exhibited enhanced antimicrobial activity due to their wider surface area related to their nano-size and effective release in media and food products [14].

Cuminum cyminum L., is a culinary spice (family Apiaceae) often used in Indian households and traditional medicine. The literature review suggests the traditional use of its seed extracts for the cure of illnesses including toothaches, dyspepsia, diarrhea, epilepsy, and jaundice, as well as for its antioxidant, diuretic, and hypoglycemic properties [15, 16]. The essential oil extracted from *Cuminum cyminum* has shown potent antioxidant and antifungal activity against post-harvest fungal pathogens such as *Botrytis cinerea*, *Aspergillus niger*, *Penicillim expansum*, *Aspergillus flavus*, and *Aspergillus parasiticus* [17, 18]. The present study aims to explore the chemical constituents of *Cuminum cyminum* essential oil (CEO) and explores the potential of chitosan nano matrix as an encapsulating agent of CEO (Ne-CEO) to boost its antifungal efficacy. The functional interaction of the CEO with the chitosan encapsulating agent was characterized using SEM and FTIR. The study also explores its probable mechanism of toxicity examining its effect on selected cellular responses including membrane function, antioxidant defenses, carbon metabolism, and transcriptional genes (Ver-1 and Nor-1) functioning of AFB_1 biosynthesis. Furthermore, the in-situ trial of Ne-CEO was also explored against the mold-mediated biodeterioration of *A. hypogaea* seed samples.

Materials and Methods

Chemicals and Instruments

The chemicals were purchased from Sigma Chemical Co. (St. Louis, MO), Hi-Media Laboratories Pvt Ltd., and SRL, Mumbai, India. Low molecular chitosan (50-190 kDa, CAS Number 9012-76-4, 75–85% deacetylated), cinnamic acid (CAS No.-140-10-3), EDC (CAS No.- 1892-57-5), aflatoxin B_1 (CAS No.- 1162-65-8) were procured from Sigma, Potato dextrose Agar (Hi-Media). The major instrument used in the study were Gas chromatography-mass spectroscopy (Perkin Elmer, Turbomass Gold, USA), Hydro-distillation unit (Merk Specialties Pvt. Ltd., Mumbai, India), Atomic Absorption spectrophotometer (Perkin Elmer, AAnalyst 800 USA), Spectrophotometer from Shimadzu (UV-1800), Colling centrifuge (CPR-24 PLUS), Probe-type Sonicator (Labman pro 500), Lyophilizer (Christ, alpha D plus), Scanning electron microscope (Evo-18 resercher, Zeiss), and Fourier transformed infrared spectrometer (Perkin Elmer, USA).

Isolated Mold Culture

The test mold species *Aspergillus flavus*, *A. niger*, *A. oryzae*, *A. ochraceus*, *Fusarium moniliformis*, *Alternaria alternata*, and *Curvularia lunata* used in this study were previously isolated by using direct plating and serial dilution methods from different food commodities [19]. The pure cultures of molds were identified and maintained in our laboratory.

Extraction and Characterization of Chemical Profile of CEO

Cuminum cyminum seed essential oil (CEO) was extracted using the hydro-distillation method following the procedure of Singh et al., 2019 [20] and the percent yield was calculated. Clevenger's device was used to extract the essential oil of CEO seed samples. The cumin seed samples (500 g) were thoroughly cleaned and added to the Clevenger flask followed by 2 L of distilled water. The samples were heated continuously for 4 h at 80 °C. Thereafter CEO was collected in clean glass tube and water residues were eliminated by adding anhydrous sodium sulfate. After removing the water traces, the oil was collected and stored in a separate glass tube for further experiments.

The chemical profile of CEO was explored using GC-MS analysis (PerkinElmer Elite-5 column (30 m length, 0.25 mm inner diameter, 0.25 mm thickness) Oven: 80 °C for 2 min, ramp 10 °C/min to 250 °C, hold 10 min, Inj = 250 °C, Split = 20:1, Carrier Gas = He, 2.00 min Solvent Delay, 180 °C Transfer, 160 °C Source, 40-400Da)

based on comparison of mass spectral patterns, and retention time (Wiley, NIST, and NBS) [21].

Preparation and Characterization of Nanogel ($CSNP_S$), and Loading of CEO (Ne-CEO)

The nanogel of CSNPs was synthesized based on the combination of cinnamic acid, EDC, and low molecular weight chitosan following the method of Beyki et al., 2014 [22]. Two different stock solutions A (by dissolving 0.5 g low mol wt. chitosan in acetic acid solution (1%)) and B (using EDC (669 µL) and 317.5 mg cinnamic acid) were prepared. The stock solution (A) was then diluted with 85 mL methanol (pH = 4) and 75 ml of this was mixed with solution B under a magnetic stirrer overnight at 250 rpm. Thereafter, its pH was adjusted to(8.5-9.0) using sodium hydroxide to precipitate the gel followed by sonication (50 Hz for 3 min), and centrifugation (9000 rpm; 10 min). The precipitates of nanoparticles ($CSNP_S$) were cleaned using distilled water and ethanol and then vacuum-dried using lyophilizer [22]. For loading of CEO, the lyophilized nanogel was re-dissolved in 1% acetic acid solution, and further different doses of CEO were added to get the concentrations ($CSNP_S$/CEO w/w at 1:0.25, 1:0.5, 1:0.75, and 1:1). The prepared CEO loaded nanoparticles were further sonicated at 50 Hz for 30 min and used for experiments.

Further, Ne-CEO was filtered through a 0.2 µm filter and then characterized by SEM and FTIR [22, 23]. In brief, a transparent and clean glass plate was coated with 10 µL of $CSNP_S$ and Ne-CEO. The dried gold-coated samples were examined for morphology characteristics using SEM analysis. The functional interaction between the CSNPs and NE-CEO was analyzed using IR spectra range (400 to 4000 cm^{-1}) [22, 23].

Encapsulation Efficiency (EE), Loading Capacity (LC) and Control Release

The method of Hasheminejad et al.,2019 [24] was used for the estimation of EE and LC. Briefly, 10 mg of Ne-CEO was added in 5 mL aqueous hydrochloric acid (2 M) at 95ºC for 30 min. Thereafter, 1 mL methanol was added to the cooled sample and centrifuged at 3000 rpm for 5 min. Similarly, the blank sample (CSNPs) was prepared. The quantity of CEO loaded inside the CSNPs was estimated using absorbance maxima (281 nm and standard curve $R^2 = 0.998$) of CEO by UV–vis spectrophotometer. The percent (%EE) and % LC were calculated following the equations:

% EE = (Mass of loaded CEO) / (Mass of initial CEO)×100.

% LC = (total amount of loaded CEO) /(Weight of freeze-dried sample) ×100.

In-vitro release of CEO from CSNPs was estimated using the sample solution (20 mg of Ne-CEO) placed in a 5 mL solution containing 60% phosphate buffer saline + 40% absolute ethanol following the methods of Hosseini et al., 2013 [25]. The mixture was vortexed and maintained at room temperature for 120 h At a regular interval (0–24 h), the solution mixture was centrifuged (11,000 rpm, 15 min) and the supernatant (200 µL) was collected to estimate the CEO release at 281 nm using a calibration curve and volume was maintain using an equal amount of PBS and 100% ethanol.

Determination of Minimum Inhibitory Concentration (MIC) Against Selected Molds and AFB_1

The PDA medium diffused with the different concentrations (0.1-1.0 µL/mL) of free CEO and Ne-CEO was inoculated (% mm disc) with selected molds species such as *Aspergillus flavus*, *A. niger*, *A. oryzae*, *A. ochraceus*, *Fusarium moniliformis*, *Alternaria alternata*, and *Curvularia lunata* and kept in BOD incubators at 27 ± 2 °C for 7 days. The MIC is recorded with no discernible growth of test molds after 7 days [26].

For AFB_1, 100 µL (10^6 spore/mL) of *A. flavus* was added to a liquid medium (SMKY) containing the desired concentration of CEO and Ne-CEO (0.1-1.0 µL/mL) and kept in a BOD incubator for 10 days. Thereafter, the mycelia were harvested and the secreted AFB_1 by the *A. flavus* (Sb-05) in liquid media was harvested by mixing of chloroform. Subsequently, the chloroform layer containing the AFB_1 was separated and evaporated in a water bath. Thereafter 5 mL methanol was added to the residue of AFB_1 and 50 µL of this was spotted on the TLC plate along with the standard of AFB_1 and developed in the solvent system (TIM: toluene (90): isoamyl alcohol (32): methanol (2) [27]. The blue color spot parallel to the standard of AFB_1 on air-dried plates was examined under a UV trans-illuminator. The fluorescent spots parallel to standard on TLC plates were scraped and dissolved in methanol subjected to 5-minute centrifugation (5000 rpm). The supernatant (OD at 360 nm) was examined using a standard equation to quantify AFB_1 following Tian et al., 2012 [28].

$$\mathrm{AFB_1\ content}\ (\mu g/\mathrm{ml}) = \frac{\mathrm{D} \times \mathrm{M}}{\mathrm{E} \times \mathrm{L}} \times 1000$$

D = absorbance; M = 312 molecular weight of AFB_1 E, extinction coefficient (21800) L = 1 cm.

Antifungal and AFB_1 Inhibitory Mechanism of Action

Determination of Ergosterol Contents and Leakage of Membrane Cations

The 50 µL (10^6 spore/mL) of *A. flavus* spore suspension was inoculated in SMKY media treated with different doses of Ne-CEO (0.1–0.4 µL/mL) was kept in a BOD incubator at 27 ± 2 °C. After 5 days incubation biomass of *A. flavus* was collected and rinsed with PBS buffer and then the wet biomass was recorded. Briefly, following 5 days incubation, the mycelia were extracted, rinsed in sterile distilled water, and then transferred to a 5 ml solution of 25% alcoholic KOH solution and vortexed for two minutes. The sample was left in the 85 °C water bath for four hours. Then, 5 ml of n-heptane and 2 ml of sterile distilled water were added to each sample. The samples were vortexed for five minutes and kept at room temperature for two hours. The n-heptane layer was collected and examined using a UV-visible spectrophotometer between 230 and 300 nm [28]. The ergosterol content was calculated using the equation:

$$\%\text{Ergosterol} = (A_{282}/290 - A_{230}/518)/W$$

A = absorbance, W = Wet biomass of *A. flavus*.

Further, atomic absorption spectrometry (AAS) was used to detect the leakages of membrane cations (Ca^{2+}, K^+, and Mg^{2+}). The *A. flavus* biomass (5 days old) was rinsed with PBS and then transferred to 0.85% saline solution (20 mL) for 12 h treated with (0.1–0.4 µL/mL). Thereafter, samples were filtered with Whatman filter paper 01, and then filtrates were used for examination of cation contents using AAS [29].

Effects of Ne-CEO on Cellular Antioxidant Defense System

The mycelia of *A. flavus* exposed to Ne-CEO (0.2 µL/mL) for 12 h were collected and crushed in liquid N_2 and PBS. The crushed mycelia were subjected to ultra-centrifugation at 15000 rpm for 10 min and the supernatant was used for the estimation of SOD (based on auto-oxidation of quercetin (406 nm) and expressed in U/mg protein), CAT (breakdown of H_2O_2, molar extinction (43.6 $mM^{-1}cm^{-1}$), and GR (at 340 nm, extinction coefficient of 6.22 mM^{-1} cm^{-1} and expressed in U/mg protein) using the methods described by Sun et al.,2016 [30] and Kumar et al. [19]. The estimation of protein was done by Bradford's method.

Investigating the Effect of Ne-CEO on the Utilization of Carbon Sources Using Biolog

The Biolog FF Microplate technique (94545, Hayward, CA) was applied to ascertain the effect of Ne-CEO on the utilization of carbon sources. Three days old *A flavus* colonies grown on PDA medium culture plates was fumigated using the appropriate doses of Ne-CEO (0.4 µL/mL) in a BOD incubator (27 ± 2 °C) along with a control plate for 4 days. Following incubation, sterile cotton swabs were used to collect *A. flavus* spores from both the treatment and control set and transferred to FF-inoculating fluid that had an adjusted 75% transmittance value. Afterward, 100 µL of this was poured into Biolog FF Microplate and cultured for 7 days in a BOD incubator. After incubation absorbance (490 nm) was recorded by Biolog plate reader (Biolog, ELx808BLG, Biotek Instrument USA) and used for the estimation of carbon source utilization [31].

Assessing the Interactive Behavior of Major Components of CEO with Selected AFB_1 Biosynthesis Gene

Using molecular docking techniques (AutoDock Vina), the predictive interactive behavior (receptor-ligand interaction) of 3D construct model of two transcriptional genes (receptor protein Ver-1 and Nor-1) of AFB_1 biosynthesis gene and major components of CEO as ligands (Cuminaldehyde, 1,3-P-Menthadien-7-Al, and 1,4-p-Menthadien-7-al) was evaluated based on binding energy [19]. Visual screening and result interpretation were also conducted in the Discovery Studio [19, 32].

Assessing the Preservative Effects of Ne-CEO in the Model food System (*Arachis hypogaea*)

The preservative effects of Ne-CEO against *A. flavus* growth, AFB_1 secretion, and lipid peroxidation using *Arachis hypogaea* were investigated using the methodology outlined by Kumar et al. [19]. To eliminate surface impurities, 500 g of A. hypogaea seed samples were sterilized (NaOCl 3%). The dried surface sterilized samples were mixed with the 5 mL (10^6 spore/mL) toxic spore of *A. flavus* before being sealed inside an airtight glass jar. Subsequently, the glass jars were fumigated with different concentrations (0.20, 0.40, and 0.80 µl/mL) of Ne-CEO for a period of six months at room temperature along with a control group that did not receive Ne-CEO fumigation. After six months of exposure, the quantity of AFB_1 was investigated with the help of standard curve eq. ($R^2 = 0.988$; $Y = 1000x + 5011$) using HPLC system equipped with a photo-diode-array detector C-18 reverse phase column (250 mm × 4.6 mm × 5 µm), mobile

phase (methanol 17: acetonitrile 19: water 64 v/v) and 1.2 mL/min flow rate [15].

Further, both control and treated sets were used for direct plating and serial dilution for the estimation of *A. flavus* colonies to estimate the percent protection from *A. flavus* growth. The MDA content (a marker for lipid peroxidation) was estimated using extinction coefficient (155 mM^{-1} cm^{-1}) and optical density at 532 nm and 600 nm [33].

Statistical Analysis

The data were generated in triplicate (Mean ± S.E.) and were analyzed by SPSS software 16.0 using one-way analysis of variance (ANOVA), P value < 0.05 was considered as significant differences using Tukey's multiple-range tests (SPSS Inc., IBM Corp.).

Results and Discussion

Isolation and Elucidation of Chemical Profile of CEO

The CEO was isolated from surface-sterilized seed samples by hydrodistillation method previously reported by our group [34]. The hydro-distillation is one of the most common and widely used methods for the isolation of essential oils from aromatic plants. After extraction, the yield (0.8%) of CEO was recorded and the chemical profile was investigated using GC-MS, revealed a total of 14 different volatile compounds comprising 94.49% of the oil (Table 1). The major components identified are cuminaldehyde (31.52%), followed by 1,4-p-Menthadien-7-al (30.59%), and 1,3-P-Menthadien-7-al (20.63%). The literature review suggested a positive correlation with the observation made in the present investigation as the cuminaldehyde was fairly reported as the major compound of CEO by other authors with variation in percent composition and some minor compounds that could be due to geographical condition, variation in seasons, plant verities, and extraction protocol [35, 36].

Table 1 Chemical composition of *Cuminum cyminum* essential oil

S.N.	Compounds	Retention time (min)	Area (%)
1.	o-Cymene	4.48	4.84
2.	Eucalyptol	4.7	0.15
3.	ç-Terpinene	4.92	5.11
4.	Timnodonic acid	6.29	0.03
5.	Terpinen-4-ol	6.77	0.13
6.	3-p-Menthen-7-al	6.96	0.85
7.	Citronellol hydrate	7.11	0.24
8.	Cuminaldehyde	7.65	31.52
9.	Phellandral	8.16	0.11
10.	1,3-P-Menthadien-7-Al	8.28	20.63
11.	1,4-p-Menthadien-7-al	8.34	30.59
12.	p-Cymen-7-ol	8.45	0.08
13.	1,4-Cyclohexadiene-1-methanol,	8.93	0.15
14.	Dolichodial	9.37	0.06
	Total		94.49

Synthesis and Characterization of Chistoan Nanoparticles (CSNPs) and Encapsulation of CEO

In brief, the method described by our group Kumar et al., 2022 [19] was used to synthesize the chitosan nanoparticles (CSNPs) and subsequent encapsulation of CEO. The CSNPs were prepared using chitosan dissolved in 1% glacial acetic acid, mixed with cinnamic acid, and EDC. A cage-like structure associated with the self-aggregation of polar heads outside (Chitosan) and non-polar heads inside (cinnamic acid) in a polar environment (water) formed due to hydrophilic and hydrophobic interaction. Thereafter, the desired concentrations of CEO (1:0.25, 1:0.5, 1:0.75, 1:1 w/w) were encapsulated inside the CSNPs using probe-type ultrasonication at 50 Hz for 30 min.

Morphology of Ne-CEO: SEM Analysis

The SEM analysis revealed that the CSNPs had a mean particle size (90.590 nm), whereas the Ne-CEO (92.357 nm) (Fig. 1a) and both were nearly spherical in shape, uniform and some extents of agglomerated lumps resembling diamonds shaped were observed that could be due to the clumping of nanoparticles and varied sonication procedure. The size of the Ne-CEO was found larger than CSNPs which might be due to the loading of the CEO inside the central region of CSNPs. Because of its small size and spherical shape, Ne-CEO offers a larger surface area, which allows more efficient release of loaded CEO in the food matrix [37].

FTIR Analysis

Figure 1b depicted the spectral peaks of chitosan (CS), CSNPs, CEO, and Ne-CEO. The specific spectra of the chitosan 1643 cm^{-1} (amide 1) and 3367–3243 cm^{-1} (amide A and B) were also observed in CSNPs with a slight shift in wave numbers 1636 and 3397 − 3289 cm^{-1} that might be occurs during the process of synthesis and sonication of prepared CSNPs based on a combination of chitosan, cinnamic acid, and EDC. Further, the large number of spectral peaks in CEO suggested the complex volatile mixture components in crude CEO. In Ne-CEO, retention of chitosan-specific spectra 1636, 3531 − 3168, and closely related peaks of CEO 1462, 1408, 1310, 1210, 1170, and 1042 suggesting the loading of CEO inside the prepared CSNPs [22, 23].

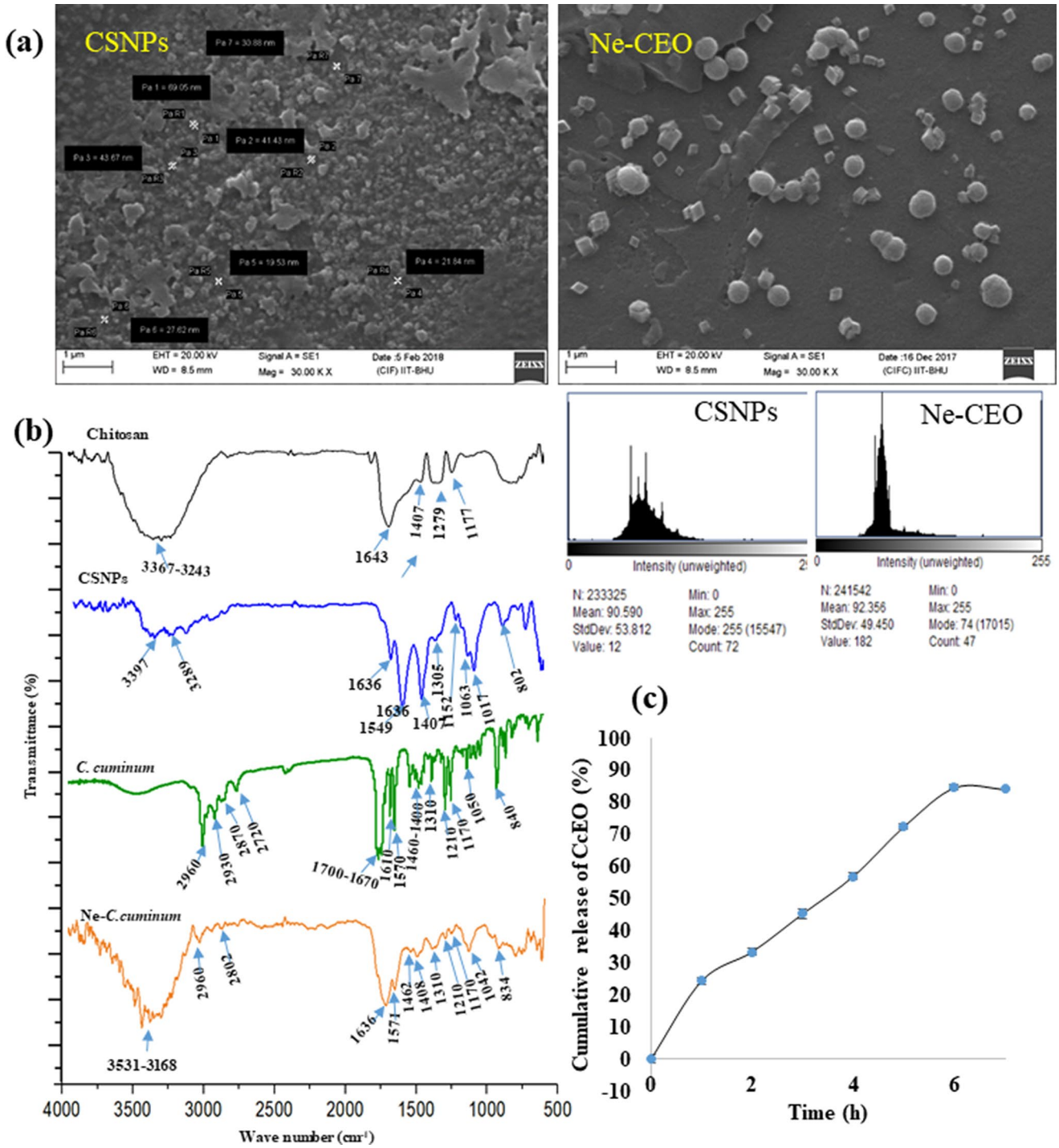

Fig. 1 Characterization of chitosan nanoparticles (CSNPs) and nanoencapsulated CEO (Ne-CEO) (**a**) SEM micrograph of CSNPs and Ne-CEO (**b**) FTIR spectra (**c**) Cumulative release

Encapsulation Efficiency (EE%), Loading Capacity (LC%) and Control Release

The percentage encapsulation efficiency (EE%), and loading capacity (LC%) at various ratios of CSNPs and CEO (w/v) were presented in Table 2. Encapsulation efficiency refers to the percentage of total available CEO encapsulated within CSNPs, whereas loading capacity refers to the amount of CEO loaded per mass of CSNPs. The results exhibited that the ratio 1:0.5 exhibited maximum EE%, whereas 1:0.75 exhibited maximum loading capacity. After this ratio, both EC and LC show a decreasing trend that could be due to the

Table 2 Encapsulation efficiency (%EE) and loading capacity (%LC) of CEO inside the chitosan nanoparticles (Ne-CEO)

CS-CEO ratio (w/w)	EE (%)	LC (%)
1: 0.25	23.86 ± 1.87^{a}	2.07 ± 0.13^{a}
1: 0.50	61.39 ± 1.17^{c}	2.66 ± 0.16^{a}
1: 0.75	55.58 ± 3.08^{c}	6.46 ± 0.30^{c}
1: 1.00	45.02 ± 2.30^{b}	4.95 ± 0.17^{b}

Value are mean ($n = 3$) ± SE. The means followed by same letter in the same column are not significantly different according to ANOVA and Tukey's multiple comparison tests

release of CEO adhere to the surface. Further, the release rate of CEO from CSNPs was investigated using a λmax with UV-spectrophotometer Fig. 1C. Initially, the CEO was released at a faster rate followed by slow release that could be associated with the aggregation and flocculation of the CEO on the surface of CSNPs. The observation was according to the previous reports that suggested the range of encapsulation efficiency percentage (40.16% and 21–47%) and loading capacity percentage (6.01% and 3–8%) for the *Artemisia annua* and *Origanum vulgare* EOs encapsulated with chitosan nanoparticles respectively [25, 38].

Determination of minimum inhibitory concentration (MIC) against molds growth and AFB_1 production of free CEO and Ne-CEO.

Figure 2a illustrates the antifungal effect of free CEO and Ne-CEO against the growth *A. flavus* in terms of inhibition of mycelia dry weight, and AFB_1 production. The minimum inhibitory concentration (MIC) value of Ne-CEO (0.4 µL/mL) for fungal growth and aflatoxin B_1 production was found to be lower than the unencapsulated CEO (0.7 µL/mL). However, the chitosan nanoparticles (CSNPs) alone did not exhibited any significant inhibition of *A. flavus* growth up to 3.0 µL/mL. In the present investigation, thin-layer chromatography (TLC) has been used for the detection of AFB_1, as it is one of the widely used analytical techniques for the estimation of AFB_1 at laboratory scale and accurate to detect at levels of 1 ng/g [39].The Rf value of AFB_1 standard and treated sets was observed at 0.71. Figure 2b summarizes the MIC values of CEO (0.6–0.8 µL/mL) and

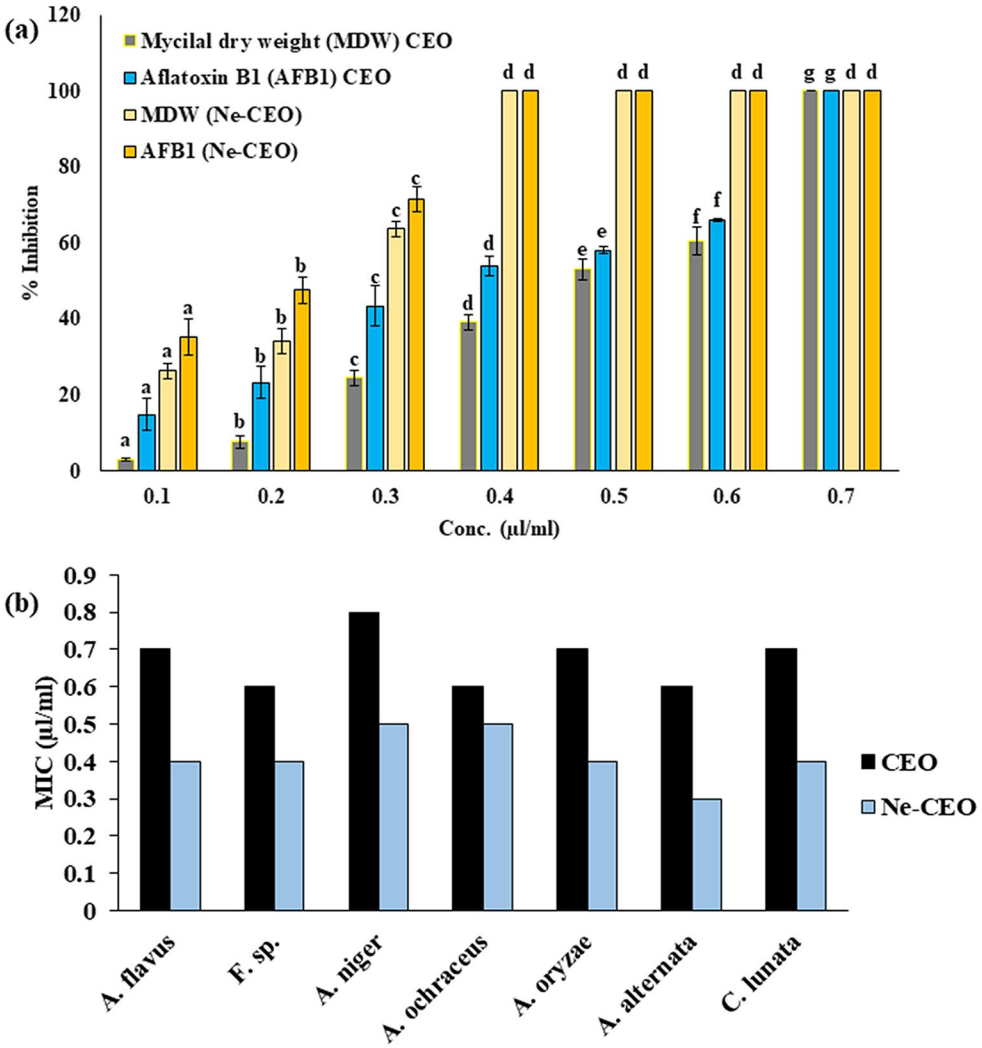

Fig. 2 (**a**)Percentage inhibition of *A. flavus* growth and aflatoxin B_1 production (**b**), Minimum inhibitory concentration of CEO and Ne-CEO against selected mold species

Ne-CEO (0.3–0.5 µL/mL) against the seven most prevalent storage molds of food commodities. The improved antifungal and AFB_1 inhibition potential of Ne-CEO over its free form could be because of the increased surface area of the nanoparticles which makes its effective attachment and entry at the cellular level. Furthermore, Ne-CEO exhibited a broad fungi toxic spectrum; hence, it could be used for the sustainable management of food-borne fungi and their associated biodeterioration.

Investigating the Antifungal and AFB_1 Inhibitory Mechanism of Ne-CEO

Ergosterol is an essential and distinctive cellular component of the fungal cell membrane and regulates cellular integrity and homeostasis, and is often used as a biomarker for determining fungal biomass [15]. The results show a remarkable decrease in ergosterol content (29.71, 43.47, and 74.94%), at different doses of Ne-CEO (0.1 to 0.3 µL/mL) Fig. 3a. Furthermore, the elevation on leakage of selected membrane cation (Ca^{++}, K^+, and Mg^{++}) was also observed (Fig. 3.b). The literature reports suggested that K^+ is a prevalent cation responsible for maintaining the charge balance, cellular homeostasis, and protein synthesis. In the present investigation, the leakage of K^+ is higher compared to other cations. Thus, the cumulative effects of a decrease in ergosterol and elevation of cation leakage lead to severe abnormalities in membrane structure and function [29] Thus, it could be concluded that Ne-CEO can disrupt the integrity of fungal cell membrane, and interfere with ergosterol biosynthesis leading to the elevation in leakage of intracellular materials (nucleic acids, lipids, and proteins), eventually leads to loss of cell's osmotic balance resulting in growth inhibition.

Furthermore, the exposure of Ne-CEO 0.2 µL/mL to *A. flavus* causes a slight increase in the SOD activity (6.64%) followed by elevation of CAT and GR (134.33% and 39.47%) enzymatic functioning has been observed (Fig. 3e, f, g). SOD is involved in the scavenging of superoxide anion (O^{2-}), CAT in the reduction of H_2O_2, and GR catalyze the reaction GSSG to GSH. The elevation in the level of cellular SOD can alter reactive hydroxyl radicals by triggering dehydrogenase activity resulting in the dysfunction of the respiratory system in the mitochondria and subsequent inhibition of aflatoxin production [40]. The elevated antioxidant defence system (CAT and GR) could be the response of cell to reduce ROS-mediated cellular damage [41].

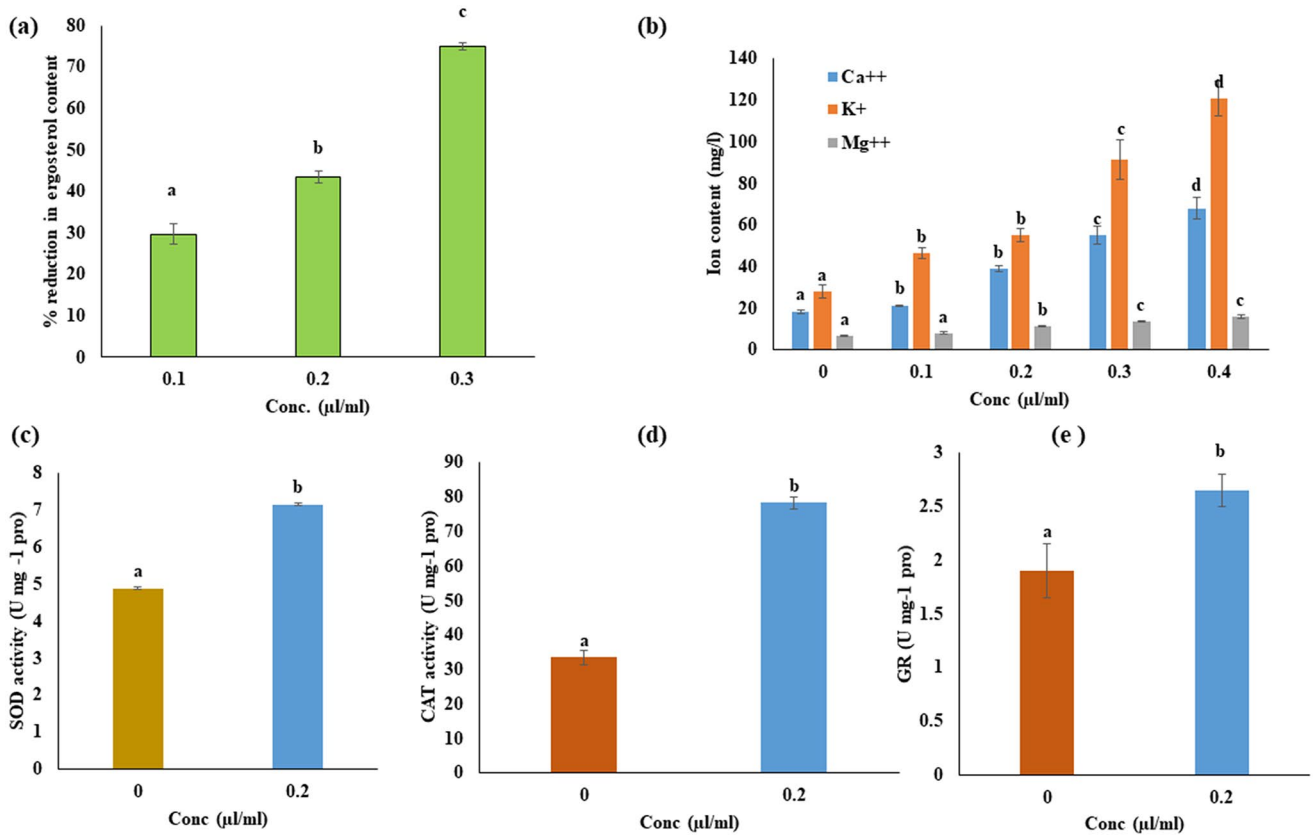

Fig. 3 Mode of action (**a**) percentage reduction of ergosterol content (**b**) Leakage of ion content (**c**, **d**, **e**) anti-oxidative defense system SOD, CAT, and, GR

The results of FF microplate Biolog test revealed that the Ne-CEO (0.4 µL/mL) alters catabolism of different carbon source in *A. flavus*. The utilization patterns of monosaccharides and disaccharides carbon sources were summarized in Fig. 4. The decrease in carbon source utilization compared to control may hamper the various biochemical pathways (Krebs cycle, pentose phosphate, and glycogen metabolism) often required for cellular growth, and metabolism [42]. Thus, it has been concluded that Ne-CEO imposes the antifungal effects associated with the damages in cell-membrane impairment in antioxidant defence and carbon source utilization patterns.

Interactive Effects of Major Compounds of CEO with the Selected Genes of AFB_1 Biosynthesis

The possible interaction of the major compounds (cuminaldehyde, 1,4-p-Menthadien-7-al, and 1,3-P-Menthadien-7-al) of CEO with the transcriptional genes (Ver-1 and Nor-1) of AFB_1 biosynthesis was explored using the molecular docking experiment. The molecular docking experiment is often used to forecast the possible interaction of selected ligands (compounds) and receptors (genes). The interaction of selected compounds of CEO and the genes responsible for aflatoxin B_1 production (Ver-1 and Nor-1) has been summarized in Fig. 5. In the biosynthetic pathway of aflatoxin B_1, the selected genes (Nor-1 and Ver-1) are accountable for the enzymatic conversion (norsolorinic acid to averantin), and (versicolorin A to dimethylsterigmatocystin which are two foremost important conversion steps in AFB_1 biosynthesis. The results show that the cuminaldehyde exhibits strong binding affinity with the targeted receptor compared to 1,3-P-Menthadien-7-Al and 1,4-p-Menthadien-7-al (Fig. 5). Hence, CEO could cause the impairment in the functioning of genes involved in AFB_1 biosynthesis. However, further study warrants conducting molecular experiments using RT-PCR to confirm the expression pattern of targeting genes using the compounds to validate the in-silico observation.

Assessing the efficacy of Ne-CEO against the *A. flavus* and AFB_1 contamination using the model food (*Arachis hypogaea*) system.

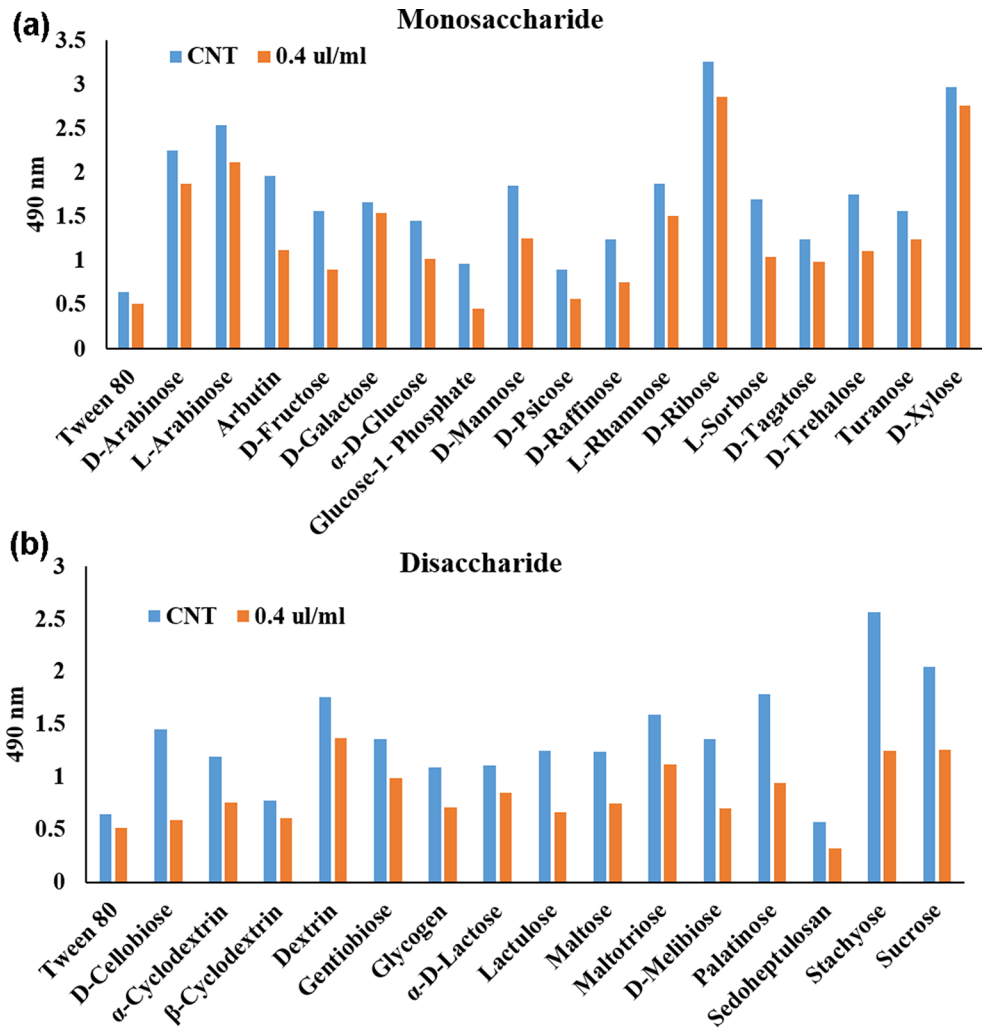

Fig. 4 Effect of Ne-CEO on carbon sources metabolism (**a**) monosaccharide C- sources (**b**) Disaccharide C- sources

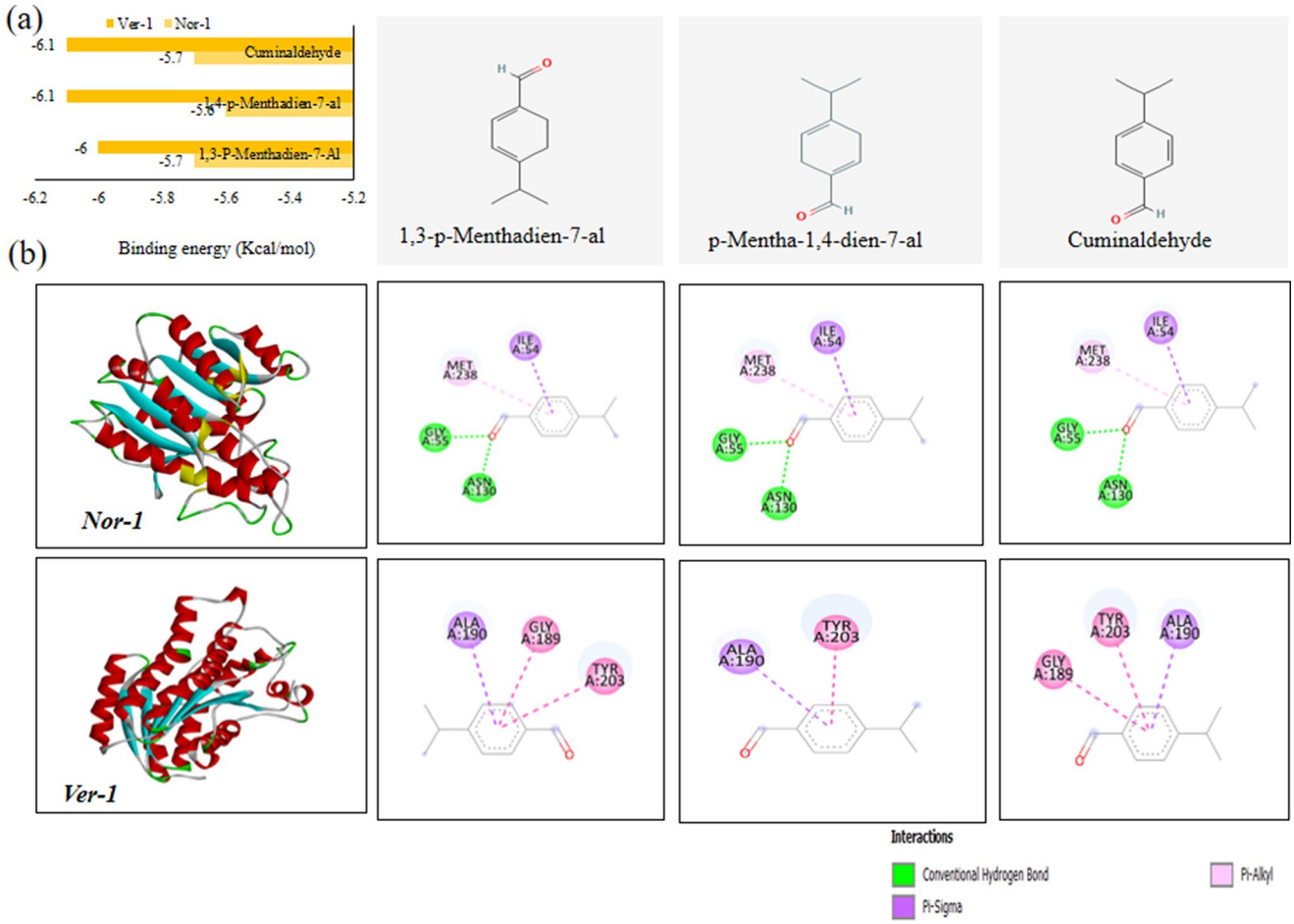

Fig. 5 In-silico interaction of major compounds of CEO with Ver-1 and Nor-1 genes involved in AFB_1 biosynthesis genes: Binding energy and ligands (**a**) interaction of ligands with different amino-acid residues (**b**)

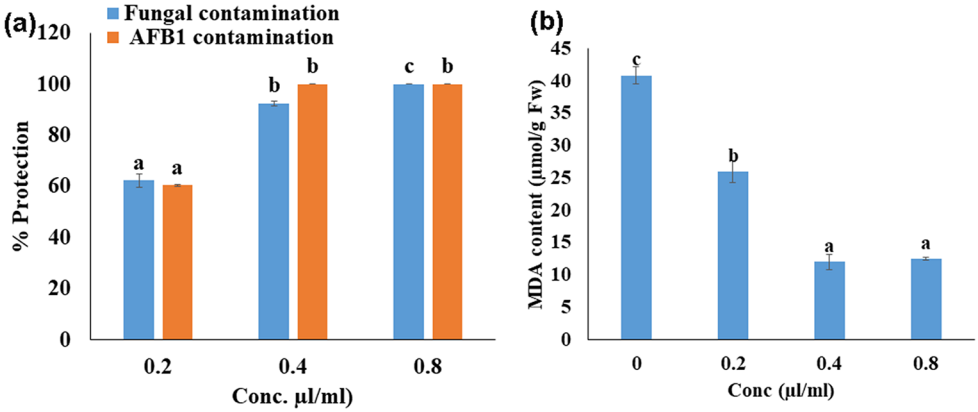

Fig. 6 In-situ practical efficacy of Ne-CEO (**a**) percentage inhibition of fungal growth and AFB_1 contamination using *Arachis hhypogea* model food system (**b**) MDA content

The potential of CEO as in-situ preservative agents for *Arachis hypogaea* seed samples against the growth and AFB_1 production by *A. flavus* has been studied and the findings are displayed in Fig. 6a, b. Ne-CEO (0.4 µL/mL) completely protected the *Arachis hypogaea* seed samples from AFB_1 contamination (100%) and *A. flavus* growth (92.27%) Fig. 6a. The malondialdehyde (MDA), a biomarker of lipid peroxidation often generate as a by-product of lipid peroxidation during the process when free radicals react with lipids (fats) in cell membranes. Hence, the presence of MDA is often used as a marker for lipid peroxidation in food system. Compared to control a sharp decline in MDA content was observed (Fig. 6b) thus, revealed the potential of CEO against the lipid peroxidation.

Conclusion

The study reports the potential of CSNPs as an encapsulating wall material for *Cuminum cyminum* essential oil (CEO) to improve its antifungal, anti-aflatoxigenic and preservative effects. In addition, a significant increase in the inhibitory effects of Ne-CEO against the growth of molds and AFB_1 has been reported compared to free CEO. The probable toxicity mechanism of Ne-CEO was linked with impairment in membrane function (decreased ergosterol and increased cation leakage), antioxidant defenses, carbon metabolism, and transcriptional genes (Ver-1 and Nor-1) involved in AFB_1 biosynthesis. Furthermore, the Ne-CEO protects the biodeterioration of *A. hypogaea* seed samples mediated through the growth of toxigenic *A. flavus*, strengthens the potential of Ne-CEO as a plant-based antifungal agent to enhance the shelf-life of food commodities. However, further studies are required regarding the effective dose standardization and their effect on organoleptic properties and nutrient profile of treated food commodities before its industrial application as a green preservative agent.

Supplementary Information The online version contains supplementary material available at https://doi.org/10.1007/s11483-024-09877-z.

Acknowledgements Authors are thankful to the Indian Institute of Technology and Department of Chemistry, Banaras Hindu University, Varanasi for SEM, and FTIR. Tanya Singh Raghuvanshi (CSIR-SRF) and Vivekanand (CSIR-JRF) are thankful to CSIR-New Delhi.

Author Contributions Credit Author StatementBhanu Prakash: Conceptualization, Supervision, Funding acquisition, reviewing, Project administrationAkshay Kumar: Experiments; Resources, Data collection, Data curation, Writing - Original DraftTanya Singh Raghuvanshi: Experiments; Resources, Data collection, Data curation, Writing - Original DraftVivekanand: Experiments; Resources, Data collection, Data curation, Writing - Original Draft.

Funding This work was supported by Banaras Hindu University Varanasi India under Institute of Eminence scheme no. R/Dev/D/IOE/Incentive/2021-22/32393.

Data Availability No datasets were generated or analysed during the current study.

Declarations

Competing Interests The authors declare no competing interests.

References

1. V. Navale, K.R. Vamkudoth, S. Ajmera, V. Dhuri, Aspergillus derived mycotoxins in food and the environment: prevalence, detection, and toxicity. Toxicol. Rep. **8**, 1008–1030 (2021). https://doi.org/10.1016/j.toxrep.2021.04.013
2. O. Civil, L. Şen, A. Demirdöven, Investigating the Effect of Glucoamylase Enzyme Treatment and Continuous Ultrasound Application on Quality Characteristics and Aflatoxins Degradation of Hazelnut Paste by Box-Behnken Response Surface Design, Food Biophysics, **19**(2), 471–489 (2024), https://doi.org/10.1007/s11483-024-09837-7
3. IARC Working Group on the Evaluation of Carcinogenic Risks to Humans, International Agency for Research on Cancer, World Health Organization, *Some Naturally Occurring Substances: Food Items and Constituents, Heterocyclic Aromatic Amines and Mycotoxins* (World Health Organization, 1993)
4. J. Ju, Y. Guo, Y. Cheng, W. Yaoc, Analysis of the synergistic antifungal mechanism of small molecular combinations of essential oils at the molecular level. Ind. Crops Prod. **188**, 115612 (2022)
5. H. Wang et al., Functional genomic analysis of aspergillus flavus interacting with resistant and susceptible peanut. Toxins. **8**(2), 46 (Feb. 2016). https://doi.org/10.3390/toxins8020046
6. A. Guimarães, A. Venancio, L. Abrunhosa, Antifungal effect of organic acids from lactic acid bacteria on Penicillium Nordicum. Food Addit. Contaminants: Part. A **35**(9), 1803–1818 (2018)
7. Y. Huang, M. Wilson, B. Chapman, A.D. Hocking, Evaluation of the efficacy of four weak acids as antifungal preservatives in low-acid intermediate moisture model food systems. Food Microbiol. **27**(1), 33–36 (2010). https://doi.org/10.1080/19440049.2018.1500718
8. Y. Wang, Q. Yang, F. Zhao, M. Li, J. Ju, Synergistic antifungal mechanism of eugenol and citral against Aspergillus Niger: Molecular Level. Ind. Crops Prod. **213**, 118435 (2024). https://doi.org/10.1016/j.fm.2009.07.017
9. B. Prakash, P.P. Singh, A. Kumar, V. Gupta, Botanicals for Sustainable Management of Stored Food Grains: Pesticidal Efficacy, Mode of Action and Ecological Risk Assessment Using Computational Approaches, Anthr. Sci., vol. 1, no. 1, pp. 62–79, Mar. 2022, https://doi.org/10.1007/s44177-022-00016-2
10. A. Coimbra, F. Carvalho, A.P. Duarte, S. Ferreira, Antimicrobial activity of Thymus zygis essential oil against Listeria monocytogenes and its application as food preservative. Innovative Food Sci. Emerg. Technol. **80**, 103077 (Aug. 2022). https://doi.org/10.1016/j.ifset.2022.103077
11. Q. Gao, J. Qi, Y. Tan, J. Ju, Antifungal mechanism of Angelica Sinensis essential oil against Penicillium Roqueforti and its application in extending the shelf life of bread. Int. J. Food Microbiol. **408**, 110427 (2024)
12. E. Niza et al., PEI-coated PLA nanoparticles to enhance the antimicrobial activity of carvacrol. Food Chem. **328**, 127131 (Oct. 2020). https://doi.org/10.1016/j.foodchem.2020.127131
13. R. De Matteo et al., Jun., Chitosan-inspired Matrices for Folic Acid. Insightful Structural Characterization and Ensured Bioaccessibility, Food Biophysics, vol. 19, no. 2, pp. 412–424, 2024, https://doi.org/10.1007/s11483-024-09833-x
14. M. Kapustová, G. Granata, E. Napoli, A. Puškárová, M. Bučková, D. Pangallo, C. Geraci, Nanoencapsulated essential oils with enhanced antifungal activity for potential application on agri-food, material and environmental fields. Antibiotics. **10**(1), 31 (2021). https://doi.org/10.3390/antibiotics10010031
15. A. Kedia, A.K. Dwivedy, D.K. Jha, N.K. Dubey, Efficacy of Mentha spicata essential oil in suppression of aspergillus flavus and aflatoxin contamination in chickpea with particular emphasis to mode of antifungal action. Protoplasma. **253**(3), 647–653 (May 2016). https://doi.org/10.1007/s00709-015-0871-9
16. S. Mnif, S. Aifa, Cumin (Cuminum cyminum L.) from traditional uses to potential Biomedical Applications. Chem. Biodivers. **12**(5), 733–742 (May 2015). https://doi.org/10.1002/cbdv.201400305
17. H. Mohammadpour, E. Moghimipour, I. Rasooli, M.H. Fakoor, S.A. Astaneh, S.S. Moosaie, Z. Jalili, Chemical composition and

antifungal activity of Cuminum cyminum L. essential oil from Alborz mountain against aspergillus species. Jundishapur J. Nat. Pharm. Prod. **7**(2), 50 (2012)
18. G. Ghasemi, M. Fattahi, A. Alirezalu, Y. Ghosta, Antioxidant and antifungal activities of a new chemovar of cumin (Cuminum cyminum L). Food Sci. Biotechnol. **28**, 669–677 (2019)
19. A. Kumar, P.P. Singh, B. Prakash, Assessing the efficacy of chitosan nanomatrix incorporated with Cymbopogon citratus (DC.) Stapf essential oil against the food-borne molds and aflatoxin B1 production in food system. Pestic. Biochem. Physiol. **180**, 105001 (2022)
20. V.K. Singh, S. Das, A.K. Dwivedy, R. Rathore, N.K. Dubey, Assessment of chemically characterized nanoencapuslated Ocimum sanctum essential oil against aflatoxigenic fungi contaminating herbal raw materials and its novel mode of action as methyglyoxal inhibitor. Postharvest Biol. Technol. **153**, 87–95 (2019). https://doi.org/10.1016/j.postharvbio.2019.03.022
21. P. Robert, Adams, Identification of Essential Oil Components by Gas Chromatography/Quadrupole Mass Spectroscopy. (2007)
22. M. Beyki, S. Zhaveh, S.T. Khalili, T. Rahmani-Cherati, A. Abollahi, M. Bayat, M. Tabatabaei, A. Mohsenifar, Encapsulation of Mentha Piperita essential oils in chitosan–cinnamic acid nanogel with enhanced antimicrobial activity against aspergillus flavus. Ind. Crops Prod. **54**, 310–319 (2014)
23. A. Barth, Infrared spectroscopy of proteins. Biochimica et Biophysica Acta (BBA)-Bioenergetics. 2007;**1767**(9):1073–1101
24. N. Hasheminejad, F. Khodaiyan, M. Safari, Improving the antifungal activity of clove essential oil encapsulated by chitosan nanoparticles. Food Chem. **275**, 113–122 (Mar. 2019). https://doi.org/10.1016/j.foodchem.2018.09.085
25. S.F. Hosseini, M. Zandi, M. Rezaei, F. Farahmandghavi, Two-step method for encapsulation of oregano essential oil in chitosan nanoparticles: Preparation, characterization and in vitro release study, Carbohydrate Polymers, vol. 95, no. 1, pp. 50–56, Jun. 2013, https://doi.org/10.1016/j.carbpol.2013.02.031
26. F. Xiang, Q. Zhao, K. Zhao, H. Pei, F. Tao, The efficacy of Composite essential oils against Aflatoxigenic Fungus Aspergillus flavus in Maize. Toxins. **12**(9), 562 (Sep. 2020). https://doi.org/10.3390/toxins12090562
27. B. Prakash, P.K. Mishra, A. Kedia, N.K. Dubey, Antifungal, antiaflatoxin and antioxidant potential of chemically characterized Boswellia Carterii Birdw essential oil and its in vivo practical applicability in preservation of Piper nigrum L. fruits. LWT - Food Sci. Technol. **56**(2), 240–247 (May 2014). https://doi.org/10.1016/j.lwt.2013.12.023
28. J. Tian, X. Ban, H. Zeng, J. He, Y. Chen, Y. Wang, The mechanism of antifungal action of essential oil from dill (Anethum graveolens L.) on aspergillus flavus. PloS One. **7**(1), e30147 (2012)
29. G.A. Helal, M.M. Sarhan, A.N.K. Abu Shahla, E.K. Abou El-Khair, Effects of Cymbopogon citratus L. essential oil on the growth, morphogenesis and aflatoxin production of Aspergillus flavus ML2-strain, J. Basic Microbiol., vol. 47, no. 1, pp. 5–15, Feb. 2007, https://doi.org/10.1002/jobm.200610137
30. Q. Sun, B. Shang, L. Wang, Z. Lu, Y. Liu, Cinnamaldehyde inhibits fungal growth and aflatoxin B1 biosynthesis by modulating the oxidative stress response of aspergillus flavus. Appl. Microbiol. Biotechnol. **100**(3), 1355–1364 (Feb. 2016). https://doi.org/10.1007/s00253-015-7159-z
31. M.P. Singh, Application of Biolog FF MicroPlate for substrate utilization and metabolite profiling of closely related fungi. J. Microbiol. Methods. **77**(1), 102–108 (Apr. 2009). https://doi.org/10.1016/j.mimet.2009.01.014
32. V.K. Raina, S.K. Srivastava, K.V. Syamasunder, Essential oil composition of Acorus calamus L. from the lower region of the Himalayas, Flavour & Fragrance J, vol. 18, no. 1, pp. 18–20, Jan. 2003, https://doi.org/10.1002/ffj.1136
33. A. Kumar, P.P. Singh, B. Prakash, Unravelling the antifungal and anti-aflatoxin B1 mechanism of chitosan nanocomposite incorporated with Foeniculum vulgare essential oil. Carbohydr. Polym. **236**, 116050 (May 2020). https://doi.org/10.1016/j.carbpol.2020.116050
34. N. Dikbas, R. Kotan, F. Dadasoglu, F. Sahin, Control of aspergillus flavus with essential oil and methanol extract of Satureja hortensis. Int. J. Food Microbiol. **124**(2), 179–182 (May 2008). https://doi.org/10.1016/j.ijfoodmicro.2008.03.034
35. C. Romagnoli, E. Andreotti, S. Maietti, R. Mahendra, D. Mares, Antifungal activity of essential oil from fruits of Indian Cuminum cyminum, Pharmaceutical Biology, vol. 48, no. 7, pp. 834–838, Jul. 2010, https://doi.org/10.3109/13880200903283715
36. A. Fattahian, A. Fazlara, S. Maktabi, M. Pourmahdi, N. Bavarsad, The effects of chitosan containing nano-capsulated Cuminum cyminum essential oil on the shelf-life of veal in modified atmosphere packaging, Food Measure, vol. 16, no. 1, pp. 920–933, Feb. 2022, https://doi.org/10.1007/s11694-021-01213-0
37. X. Jiang et al., Chitosan nanoparticles loaded with Eucommia ulmoides seed essential oil: Preparation, characterization, antioxidant and antibacterial properties. Int. J. Biol. Macromol. **257**, 128820 (Feb. 2024). https://doi.org/10.1016/j.ijbiomac.2023.128820
38. M. Mojarab-Mahboubkar, Z. Afrazeh, R. Azizi, J.J. Sendi, Efficiency of Artemisia annua L. essential oil and its chitosan/tripolyphosphate or zeolite encapsulated form in controlling Sitophilus oryzae L., Pesticide Biochemistry and Physiology, vol. 195, p. 105544, Sep. 2023, https://doi.org/10.1016/j.pestbp.2023.105544
39. P.K. Mishra, R. Shukla, P. Singh, B. Prakash, N.K. Dubey, Antifungal and antiaflatoxigenic efficacy of Caesulia Axillaris Roxb. Essential oil against fungi deteriorating some herbal raw materials, and its antioxidant activity. Ind. Crops Prod. **36**(1), 74–80 (2012)
40. T. Furukawa, S. Sakuda, Inhibition of Aflatoxin Production by Paraquat and External Superoxide Dismutase in Aspergillus flavus, Toxins, vol. 11, no. 2, p. 107, Feb. 2019, https://doi.org/10.3390/toxins11020107
41. T.-L. Wu et al., Antifungal efficacy of sixty essential oils and mechanism of oregano essential oil against Rhizoctonia solani. Ind. Crops Prod. **191**, 115975 (Jan. 2023). https://doi.org/10.1016/j.indcrop.2022.115975
42. K.M. Geyer, E. Kyker-Snowman, A.S. Grandy, S.D. Frey, Microbial carbon use efficiency: accounting for population, community, and ecosystem-scale controls over the fate of metabolized organic matter. Biogeochemistry. **127**, 2–3 (Feb. 2016). https://doi.org/10.1007/s10533-016-0191-y